Characterization of dextrans produced by *Lactobacillus mali* CUPV271 and *Leuconostoc carnosum* CUPV411

María Goretti Llamas-Arriba[a], Ana I. Puertas[a], Alicia Prieto[b], Paloma López[b], Mónica Cobos[a], José I. Miranda[a], Cristina Marieta[a], Patricia Ruas-Madiedo[c], and Mª Teresa Dueñas[a]

[a]University of Basque Country (UPV/EHU), San Sebastián, Spain.
[b]Biological Research Centre (CIB), Spanish National Research Council (CSIC), Madrid, Spain.
[c]Asturias Dairy Centre (IPLA), Spanish National Research Council (CSIC), Villaviciosa, Spain.

*** Correspondence:**
Mª Teresa Dueñas
mariateresa.duenas@ehu.eus

Keywords: dextran, *Lactobacillus*, *Leuconostoc*, characterization, adhesion.

Abstract

The exopolysaccharide (EPS)-producing *Lactobacillus mali* CUPV271 and *Leuconostoc carnosum* CUPV411 were isolated from Spanish ropy apple must and slimy ham, respectively. The polymers were purified from bacterial cultures' supernatants and subjected to physicochemical and rheological characterization with the aim to evaluate their potential for future industrial utilization. Methylation analysis, Fourier-Transform Infrared Spectroscopy (FT-IR) and Nuclear Magnetic Resonance (NMR) revealed that both polymers were dextrans, partially branched at *O*-3 and *O*-4 positions of the main α-(1→6)-D-glucopyranose backbone. The molar masses of the EPS of *L. mali* and *Lc. carnosum*, were of 1.23 x 10^8 g/mol and 3.58 x 10^8 g/mol, respectively. The bacterial strains were tested for binding to the human Caco-2 cell line in the presence and absence of their respective dextran, revealing that the EPS production by *L. mali* decreased the binding capacity of the bacterium while the adhesiveness of *Lc. carnosum* did not change. As the structure and molecular mass of both dextrans were comparable, other characteristics of the dextrans were studied to explain this behavior. Atomic force micrographs showed some differences at the supramolecular level, suggesting that the different spatial distribution of the dextrans might be on the basis of the results of the adhesion studies. Both polysaccharides resulted to be amorphous materials with T_g around 226 °C and showed slightly different thermal degradation patterns. Rheologically, they showed to have a pseudoplastic behavior, but very different critical concentrations: 3.8% for the EPS of *L. mali* and 0.4% for that of *Lc. carnosum*.

1. Introduction

Lactic acid bacteria (LAB) can produce a variety of EPS, either homopolysaccharides (HoPS), with a single type of sugar monomer, or heteropolysaccharides (HePS), made up by two or more different monosaccharides (Torino, Font de Valdez, & Mozzi, 2015). LAB are considered good glucan-producers, and among these HoPS, specifically, they synthesize α-glucans, which are composed of α-glucose. Dextrans are classified within this group and are composed of a main chain of α-(1→6)-linked glucopyranose units, which can be branched by α-(1→2), α-(1→3) or α-(1→4) linkages, in a proportion lower than 50%. Dextrans' production by LAB is not always desirable, for example, when they form the slime film that spoils meat products, although in general dextrans help to obtain better products. For instance, they can improve the texture, rheology and

palatability of some beverages, and they serve as cryoprotectants or moisture-increasers (Lakshmi Bhavani & Nisha, 2010). In addition, they can be produced *in situ* in fermented dairy food, developing their prebiotic role, or during sourdough fermentation to improve texture and storage life of bread (Hu & Gänzle, 2018; Kothari, Das, Patel, & Goyal, 2014). Moreover, dextrans are applied in other fields than food industry. They have been reported as having antiviral activity in salmonids, to serve as plasma substitutes or as coating for columns with separation purposes (Chang, Crawford, & West, 1980; Lakshmi Bhavani & Nisha, 2010; Nácher-Vázquez et al., 2015; Pérez-Ramos, Nácher-Vázquez, Notararigo, López, & Mohedano, 2015). In 1878, Van Tiehem described the first microorganism responsible for dextran production and named it *Leuconostoc mesenteroides* (Meng et al., 2016). Since then, a lot of different bacteria have been isolated as dextran-producers, from other *Leuconostoc* to *Lactobacillus*, *Weissella*, *Streptococcus* or *Oenococcus* species (Dimopoulou et al., 2014; Dueñas-Chasco et al., 1998; Hu & Gänzle, 2018; Nácher-Vázquez et al., 2015; Vuillemin et al., 2018; Zarour et al., 2017). Dextrans are synthesized from sucrose by dextransucrases, a type of glucansucrases mostly belonging to the glycoside hydrolase family 70 (Meng et al., 2016). Depending on the linkage specificity of the dextransucrase, dextrans are different in branches and proportion. Thus, depending on each bacterium and its specific dextransucrase, dextrans can be different one from another. Still nowadays, the most used dextran in industry is that produced by *Lc. mesenteroides* NRRL B-512F, with a 95% of α-(1→6) glucosidic linkages (Naessens, Cerdobbel, Soetaert, & Vandamme, 2005). However, the multiple applications of dextrans, as well as the increasing demand on free-additive products, make necessary the search for new dextran-producers. Thus, the aim of this work was the isolation of dextran-producing bacteria from different food origins and the characterization of the dextrans they produce.

2. Materials and Methods

2.1. Bacterial strains and growth conditions

Two LAB strains were isolated, respectively, from the ropy slime of the surface of a vacuum-packed sliced cooked ham and from an apple must from a Spanish cider producer (Basque Country) as follows. Serial dilutions in Ringer's solution of the slime and the apple must were cultivated in MRS (De Man, Rogosa, & Sharpe, 1960) agar plates (pH 6.0), containing 2 µL/mL pimaricin and 5% sucrose, at 28 °C under a

microaerophilic atmosphere (CampyGen™, ThermoScientific) for 24 h. These bacteria were identified as *Leuconostoc carnosum* CUPV411 and *Lactobacillus mali* CUPV271 by sequencing a fragment of their 16 rRNA coding genes at Secugen (Madrid, Spain). The data were deposited in GenBank with accession numbers MH628089 and MH628046, respectively. LAB were grown at 30 °C without shaking in MRS medium containing either 2% glucose (MRSG) or 2% sucrose (MRSS). The media were buffered at pH 6.8 or 5.5 for growth of either *Lc. carnosum* or *L. mali*. The strains were stored in MRSG containing 20% (v/v) glycerol at –80 °C. For EPS production, a semi-defined (SMD) medium containing 2% sucrose (SMDS) and no glucose (Dueñas-Chasco et al., 1997) was used with the aim of avoiding the contamination with polysaccharides present in the MRS medium.

2.2. Production, purification and quantification of EPS from LAB

First, *L. mali* and *Lc. carnosum* were grown in MRSS for 24 h and the bacterial cultures were used as inoculum for further growth in SMDS medium at pH 5.5 and 6.8 respectively, for 48 h at 28 °C in a 5% CO_2-atmosphere. Then, the bacteria were sedimented by centrifugation (18500 x *g*, 4 °C, 10 min) and the EPS were recovered from the supernatants by precipitation with 1 volume of cold ethanol for 15 h at -20 °C. Afterwards, EPS were sedimented by centrifugation (18500 x *g*, 4 °C, 15 min), dialysed in 12-14 kDa MWCO membranes (Iberlabo) against distilled water for 3 days, freeze-dried and kept at room temperature. Finally, lyophilised EPS were dissolved in ultrapure water (0.1 mg/mL) and their concentration was determined from their neutral carbohydrate content, quantified by the phenol-sulphuric acid method (Dubois, Gilles, Hamilton, Rebers, & Smith, 1956) using glucose as standard.

2.3. Monosaccharide composition, methylation and FT-IR analyses

With the aim of elucidating the type of EPS isolated from the two strains neutral sugar composition and linkage types were determined as previously described (Notararigo et al., 2013). Neutral sugars were identified and quantified by gas chromatography, after hydrolysis of polysaccharides' samples with 3 M trifluoroacetic acid (TFA) for 90 min and derivatization to alditol acetates. To determine linkage types, the polysaccharides were methylated according to Ciucanu and Kerek (Ciucanu & Kerek, 1984), hydrolyzed with TFA 3 M for 1 h at 120 °C, converted into partially methylated alditol acetates using sodium borodeuteride as the reducing agent and analyzed by gas-

chromatography/mass spectrometry. The linkages in the polysaccharides were deduced from the mass spectra and retention time of the peaks, and their relative amount from the area under each peak. For Fourier-Transformed Infrared Spectroscopy (FTIR) analysis, KBr pellets of the samples were first prepared, recording the spectra in a FTIR 4200 instrument (Jasco Corporation) in the range 4000-700 cm^{-1}. The number of scans per experiment was 50, with a resolution of 4 cm^{-1}.

2.4. NMR spectroscopy analysis

Samples were weighted (*ca.* 1 mg) and dissolved 1:1 (w/v) in D_2O and their spectra were recorded at 333 K on a Bruker Avance NEO spectrometer operating at 500.13 MHz (^1H) and 125.75 MHz (^{13}C), BBOF probe with z-gradients. Chemical shifts are given in ppm, using the acetone signal (2.16 ppm) (^1H) and (30.7 and 215.7 ppm) (^{13}C) as reference. To record the 1D spectra, solvent suppression (WATERGATE) was used. The homonuclear COSY spectra were recorded using a presaturation to remove the residual signal of solvent (3K x 512 increments) with 8 scans. The heteronuclear single quantum coherence spectroscopy (HSQC) with solvent suppression was performed (2K x 256 increments) with 128 scans. The heteronuclear multiple bond correlation (HMBC) experiment was performed (4K x 256 increments) with 128 scans. To improve the sensitivity, a BBI with z-gradient probe was used to record the HSQC and HMBC spectra.

2.5. Detection of dextrans' production at cellular level

For phenotypic determination at cellular level, LAB cultures were grown in MRSG liquid medium to A_{600} = 1.0. Then, 100 µL of appropriate dilutions were streaked on MRSS- and MRSG-agar plates and incubated for 11 days. The detection of EPS in the LAB colonies was performed by transmission electron microscopy (TEM). Three or four colonies of each strain from MRSS- and MRSG-agar plates were carefully suspended in 50 µL of sterile distilled water to form a turbid suspension, which was subjected to negative staining with uranyl acetate, prior TEM analysis as previously described (Zarour et al., 2017).

2.6. Caco-2 cell culture and adhesion assays

The Caco-2 human enterocyte cell line, obtained from the cell bank at Centro de Investigaciones Biológicas (CIB, Madrid, Spain), was seeded in 96-well tissue culture

plates (Falcon Microtest™) at a final concentration of 1.25 x 10^5 cells/mL, and grew as monolayers of differentiated and polarized cells as previously described (Nácher-Vázquez et al., 2017). Cell concentrations were determined as previously described (Garai-Ibabe et al., 2010). For adhesion assays, LAB, grown in MRSG and MRSS to the middle of the exponential-phase cultures, were diluted to a final volume of 1 mL of DMEM (Invitrogen) supplemented with 0.5% of glucose or 0.5% sucrose, to give 1.25 × 10^6 colony-forming units (cfu)/mL, and added to Caco-2 cells (ratio 10:1, bacteria:Caco-2 cells) in a final volume of 0.1 mL per well. After incubation for 1 h at 37 °C in a 5% CO_2 atmosphere, unattached bacteria were removed by washing three times with 0.2 mL of phosphate buffered saline (PBS) solution at pH 7.2 and then, Caco-2 cells were detached from the plastic surface by incubating for 5 min at 37 °C with 0.1 mL of 0.05% trypsin–EDTA per well. The detachment reaction was stopped by adding 0.1 mL of PBS pH 7.2. To determine the number of cell-associated bacteria, appropriate dilutions were plated onto MRSG-agar plates. All adhesion assays were conducted in triplicate, with two biological replicates in each.

2.7. Physicochemical characterization of the isolated dextrans

2.7.1. Determination of the molar mass distribution by SEC-MALLS

The molar mass distribution of the purified dextrans was analyzed by means of size exclusion chromatography coupled with multiangle laser light scattering detection (SEC-MALLS) as previously described (Nikolic et al., 2012). In short, each lyophilized sample was resuspended in 0.1 M $NaNO_3$ at a concentration of 5 mg/mL, kept overnight under gentle stirring and centrifuged (10,000 × *g*, 10 min) before analysis. The HPLC system (Waters, Milford, MA) consisted of a separation module Alliance 2695 connected with two detectors: a refractive index (RI 2414, Waters) to determine the amount of dextran using calibration curves obtained from standards of dextran (Fluka-Sigma, St. Louis, MO), ranging from 5 × 10^3 to 4.9 × 10^6 Da (Salazar et al., 2009), and the MALLS Dawn Heleos II (Wyatt Europe GmbH, Dembach). The quantification of dextrans was achieved with the Empower software (Waters) and the molar mass distribution analysis with the Astra 3.5 software (Wyatt Europe GmbH). Two SEC columns placed in series were used: TSK-Gel G3000 PW_{XL}+TSK-Gel G5000 PW_{XL} protected with a TSK-Gel guard column (Supelco-Sigma) and the separation was carried out at 40 ºC with a flow rate of 0.45 mL/min using 0.1 M of $NaNO_3$ as mobile phase.

2.7.2. Thermal analysis

Thermogravimetric analysis (TGA) was carried out using a thermogravimeter Q-500 (TA Instruments), under dynamic nitrogen and air atmospheres (90 mL/min) at a heating rate of 10 °C/min, within the temperature interval from room temperature to 580 °C. Samples were weighted (between 8 and 14 mg) in a platinum pan.

2.7.3. Analysis by differential scanning calorimetry (DSC)

DSC curves were obtained from samples between 9 and 12 mg in aluminum crucibles under a nitrogen atmosphere flowing at 3 mL/min, in a differential scanning calorimeter DSC 3+ (Mettler Toledo). Samples were first maintained at -30 °C during 3 min. Then, two heating scans separated by a cooling stage at 10 °C/min were performed. The first heating scan was performed to erase the thermal history of the materials as reported previously (Fernández, Fernández, & Cobos, 2016; Icoz & Kokini, 2007), and was raised from -30 °C to 210 °C, maintaining the temperature for 5 min at the end. In the cooling stage, the temperature fell to -30 °C and was maintained for 3 min. Finally, in the second scan 300 °C were reached.

2.7.4. X-ray diffraction (XDR) analysis

The identification of the crystalline and/or amorphous structure of the purified dextrans was analyzed. The X-ray powder diffraction patterns were collected by using a PHILIPS X'PERT PRO automatic diffractometer operating at 40 kV and 40 mA, in theta-theta configuration, secondary monochromator with Cu-Kα radiation (λ = 1.5418 Å) and a PIXcel solid-state detector (active length in 2θ 3.347º). Data were collected from 5 to 60° 2θ (step size = 0.026 and time per step = 90 s) at room temperature, 0.04 rad soller slit and variable divergence slit giving a constant 5 mm area of sample illumination.

2.7.5. Atomic force microscopy (AFM) analysis

Aqueous solutions of the two dextrans were prepared at 1 mg/mL with filtered (0.45 μm) deionized water and kept *ca*. 16 h to assure solubilization. Then, serial dilutions were made to obtain a final concentration of 1 μg/mL. About 5 μL of this solution were dropped onto a cleaved mica substrate and allowed to dry at room temperature for 24 h in a desiccator. AFM images were obtained with a NanoScope V microscope (Digital

Instruments) operating in tapping mode, with 512 x 512 pixels, and TESP 0.01-0.025 ohm-cm Antimony (n) doped Si tips (T=3,8 μm, f_0=320 kHz) (Bruker). As a contrast enhancement technique (Corcuera et al., 2010), phase imaging extension was used. Scan rates ranged from 1 to 2 Hz.

2.8. Rheological analysis

The rheological behavior of the two dextrans was determined as previously described (Zarour et al., 2017). Briefly, the lyophilized EPS were dissolved in ultrapure water at different concentrations, stirring at room temperature and then allowing them to settle overnight before each analysis. The viscoelastometer used was a Thermo-Haake Rheostress I (ThermoFisher Scientific), equipped with a cone-plate (60 mm diameter, 2° cone angle) geometry. Each solution (2 mL) was measured in two steps: the first one consisted on 3 min of resting without shear to maintain the temperature at 20 °C. Then, an interval shear-rate range was applied for 3 min between 1 and 500 s^{-1}. Each experiment was repeated at least three times. Haake Rheowin Data Manager was used for analyzing the continuous steady-state flow from the apparent viscosity and shear rate relationship. Viscosity at shear near zero (η_o) was extrapolated and regressed using the Cross model (Cross, 1965).

2.9. Statistical analysis

Adhesion data were analyzed by two-way analysis of variance (ANOVA) to determine the significant differences between the variables at $p \leq 0.05$. The analysis was performed using the SAS 9.4 software (SAS Institute Inc).

3. Results and discussion

3.1. Elucidation of the type of EPS produced by *L. mali* CUPV271 and *Lc. carnosum* CUPV411

The EPS produced by the two LAB were purified from the supernatants of 48 h-cultures and analyzed to determine their composition and structure. Both EPS contained glucose as the sole monosaccharide, indicating that they produced a glucan-type HoPS.

Their FT-IR spectra were very similar (Figure 1), with absorption bands typical of polysaccharides (Salazar, Ruas-Madiedo, Prieto, Calle, & de los Reyes-Gavilán, 2012), In the anomeric region, the bands at 917 and 844 cm^{-1}, characteristic of α-anomers (Heyn, 1974), and the absence of bands characteristic of β-linkages, indicated that they

are α-glucans. The results from this analysis also confirmed the absence of non-glucidic components (phosphates, sulphates, protein) in the polysaccharides analyzed.

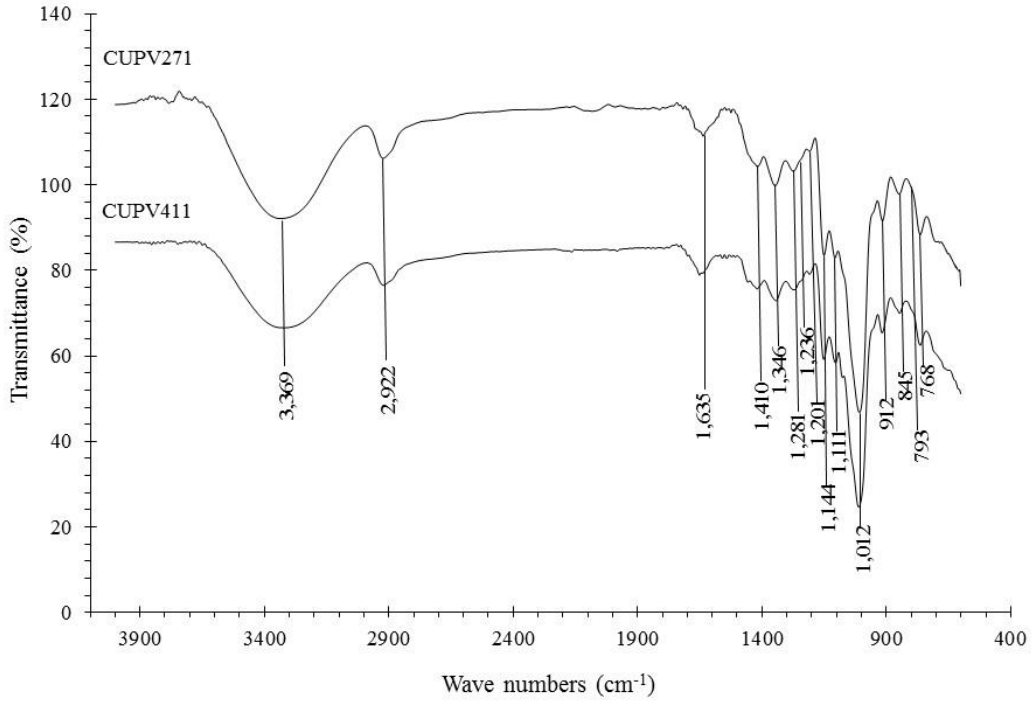

Fig. 1. FT-IR spectra of isolated dextrans. Up, spectrum of the HoPS from *Lactobacillus mali* CUPV271 and down, the spectrum of the dextran isolated from *Leuconostoc carnosum* CUPV411.

Methylation analysis (Table 1) showed the predominance of linear residues of (1,6)-glucopyranose in the structure of both polymers as well as the presence of 3,6-di-*O*-substituted glucopyranose (branching points) and terminal units of glucopyranose that amounted to 3.6% in the polysaccharide from *L. mali* and to 6.8% in that of *Lc. carnosum*. These data, together with the α-configuration of the linkages deduced from FT-IR, suggest that these polysaccharides are dextrans. Commercial dextrans have branching degrees around 5%, and the side chains are mainly composed of single α-D-glucopyranosyl units (about 40%), or are two units long (about 45%), while only 15% of them contain more than 2 units (BeMiller, 2003). Therefore, the small percentage of linear units of glucose (1,3)-linked detected in the methylation analysis may belong to the short side-chains in the dextran structure. Around 1.5% of substitutions at positions *O*-4 were also detected in the two polysaccharides, which is more unusual, as this type

of dextrans, branched at positions other than *O*-3, have been reported in few cases (Fraga Vidal, Moulis, Escalier, Remaud-Siméon, & Monsan, 2011).

Table 1. Linkage types and their percentages deduced from methylation analysis of dextrans synthesized by *L. mali* CUPV271 and *Lc. carnosum* CUPV411.

Linkage type	Rt (min)	%	
		***L. mali* CUPV271**	***Lc. carnosum* CUPV411**
Glc*p*-(1→	6.9	3.6	6.8
→3)-Glc*p*-(1→	8.9	2.1	0.7
→6)-Glc*p*-(1→	9.9	84.8	81.1
→4,6)-Glc*p*-(1→	12.1	1.6	1.5
→3,6)-Glc*p*-(1→	12.4	7.9	9.9

For further confirmation of the methylation data, the both polysaccharide samples were analyzed by NMR spectroscopy, revealing very similar ^{1}H NMR and ^{13}C NMR spectra among them. The anomeric proton resonances for the ^{1}H NMR spectra (Figure 2) of the polymers coincide with those reported for 1,3-branched dextrans as the B-1351 dextran (Cheetham, Fiala-Beer and Walker, 1990). A main anomeric signal at 4.91 ppm (coupling constant J= 3.7 Hz) attributable to the α-(1→6)-glucopyranose linkages of the dextran backbone, and a small anomeric signal at 5.25 ppm, were observed in the anomeric region. Integration of the area of both peaks gave a ratio of 5.6/94.4, which also supports the data deduced from methylation analysis. The signals between 3.2-4.4 ppm correspond to the protons of the monosaccharides' backbone (Polak-Berecka et al., 2015). The ^{13}C NMR spectra of the polysaccharides (Figure 3) showed a single anomeric signal from the α-(1→6)-glucopyranose backbone at 98.3 ppm (Miao et al., 2016), confirming that the EPS contained α-anomeric carbons instead of β-anomeric carbon atoms with resonances downfield from 102 ppm (Seymour, Knapp, Chen, Jeanes, & Bishop, 1979), as we deduced from the FT-IR analysis. However, the signals of the anomeric carbon of the α-glucose branches were not observed in the ^{13}C spectrum.

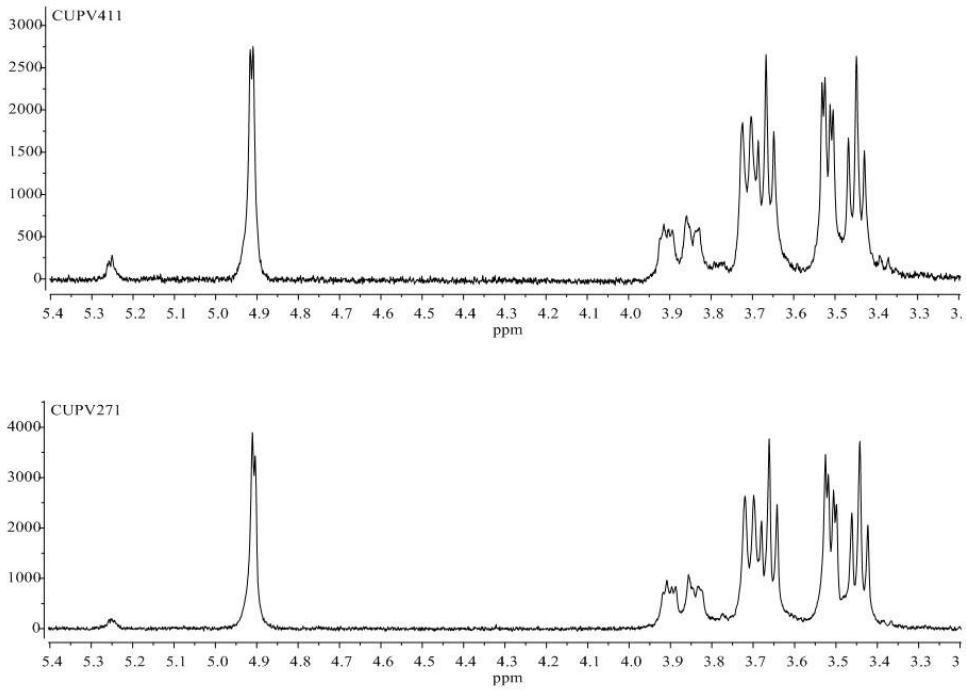

309 **Fig. 2.** [1]H NMR spectra of CUPV411 strain (up) and CUPV271 strain (down).

310

311

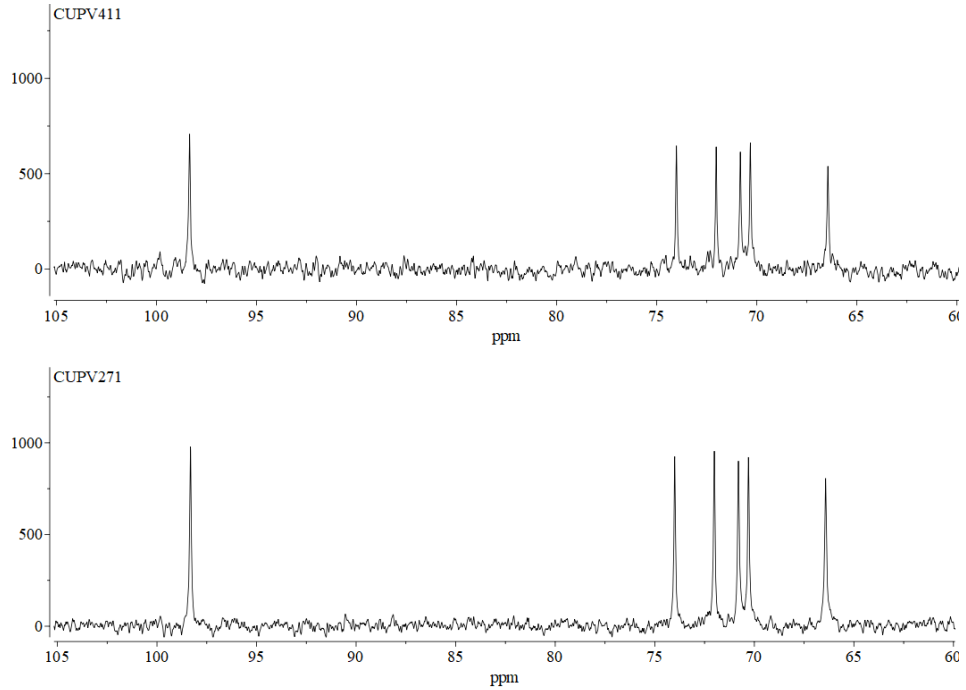

312

313 **Fig. 3.** 13C NMR spectra of CUPV411 strain (up) and CUPV271 strain (down).

314

315

The assignment of ^{1}H and ^{13}C resonances of the main monosaccharide (Table 2) was performed on the basis of homonuclear COSY (Figure 4A) and heteronuclear HSQC (Figure 4B) two-dimensional correlation NMR experiments. The system with ^{1}H anomeric signal at 5.25 ppm could not be assigned, although analysis of various dextrans has shown that this signal is characteristic of α-(1→3) branched dextrans, (Cheetham, Fiala-Beer, & Walker, 1990; Dertli, Colquhoun, Côté, Le, & Narbad, 2018; Miao et al., 2016; Seymour, Knapp, & Bishop, 1979), which also coincide with our methylation results. The HMBC spectrum (Figure 5) confirmed the α-(1,6) linkage through the correlation between H6 and H6' signals (3.90 ppm and 3.72 ppm, respectively) and C1 signal (98.3 ppm). In addition, the overlap of the HSQC and HMBC spectra (data not shown) only gave information on the (1→6) linkage through the correlation of H1-C1 signals (4.91-98.3 ppm) with the two protons of C6 (H6: 3.90 ppm and H6': 3.72), but signals from the minor components of the polysaccharide were not observable in any of the spectra analyzed. Thus, the presence of the α-glucopyranose side chains could not be confirmed with the experiments performed, although the ^{1}H NMR spectra (Figure 2) showed a signal which could be interpreted as corresponding to one of them.

Table 2. ^{1}H and ^{13}C NMR chemical shifts (ppm) for the main monosaccharide α-(1→6)-glucopyranose.

	H-1	**H-2**	**H-3**	**H-4**	**H-5**	**H-6**	**H-6'**
^{1}H	4.91	3.51	3.61	3.44	3.85	3.90	3.72
^{13}C	98.3	72.0	74.0	70.3	70.8	66.5	66.5

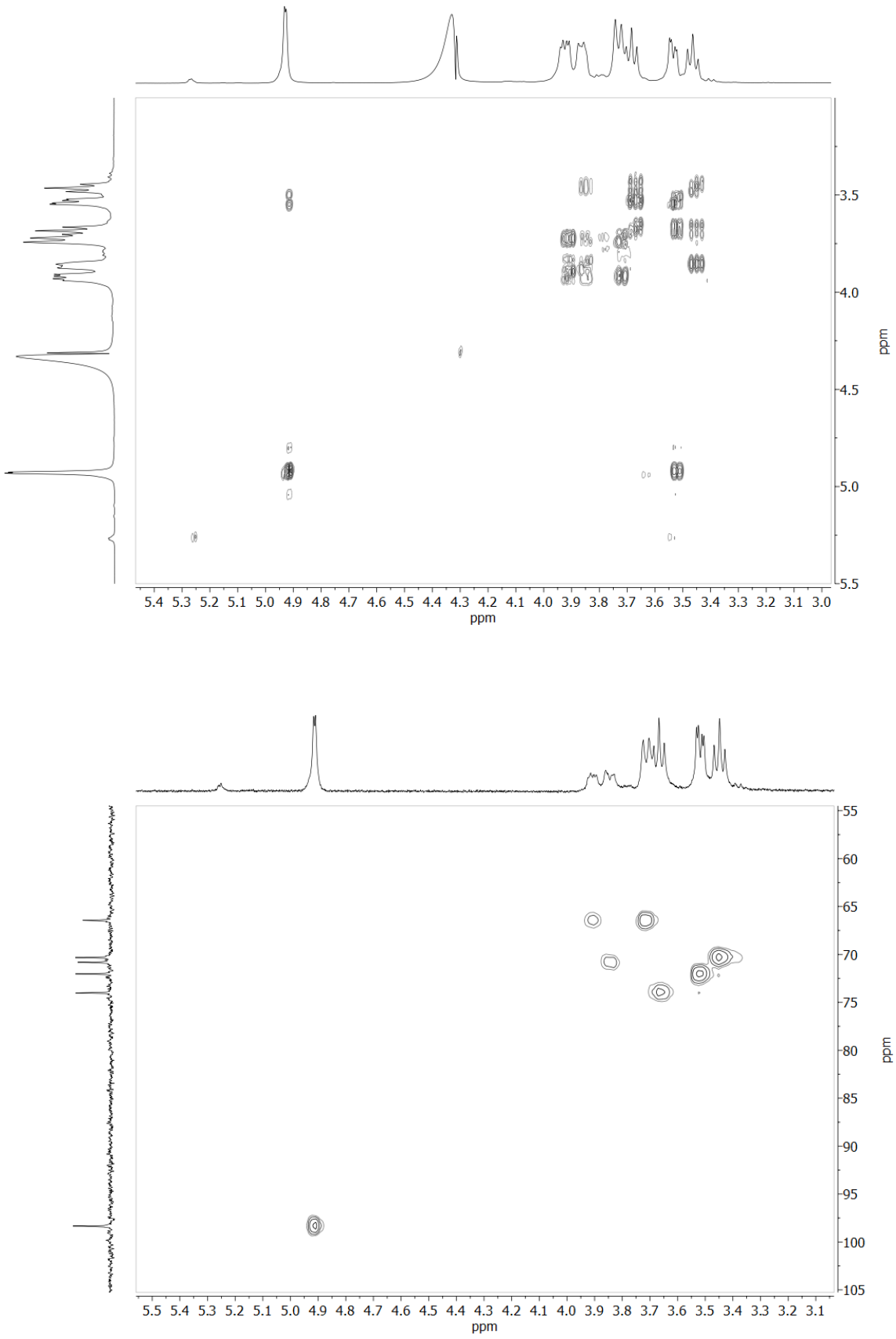

Fig. 4. 2D-NMR analysis of dextran produced by CUPV411 strain. (A) ^{1}H-^{1}H COSY spectrum and (B) ^{1}H-^{13}C HSQC spectrum.

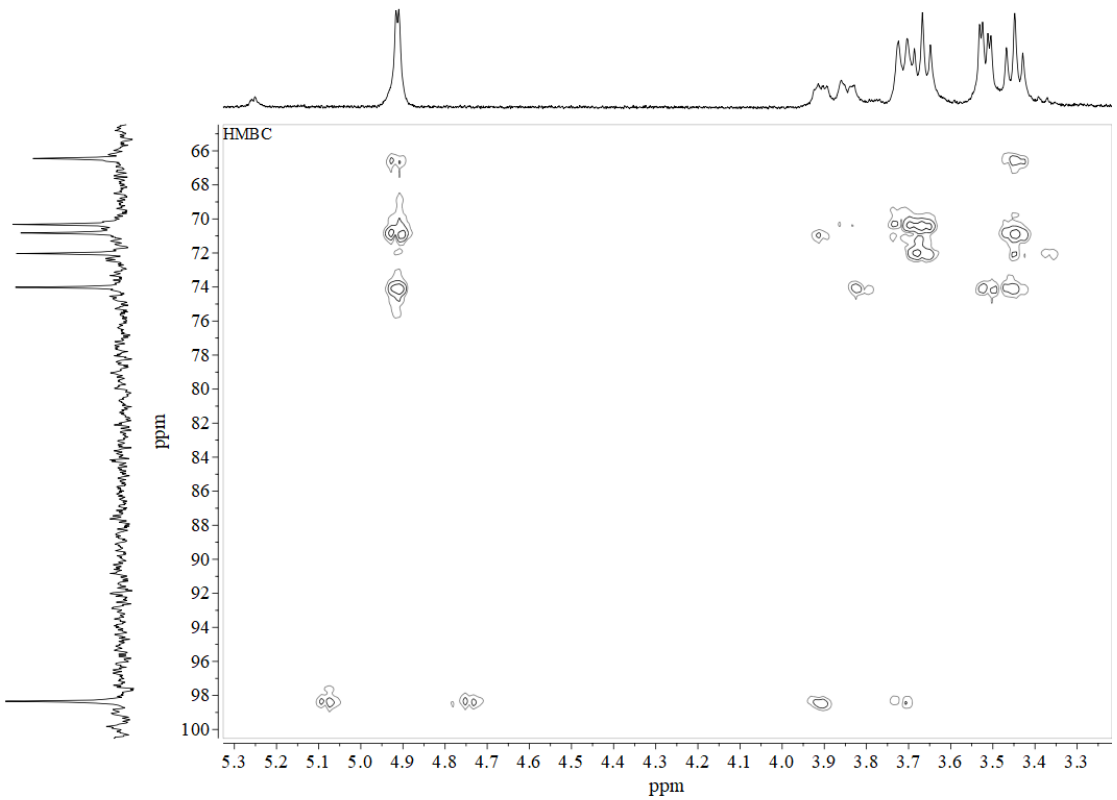

Fig. 5. HMBC spectrum of *Leuconostoc carnosum* CUPV411.

The scheme 1 represents the main linkage types in the *Lc. carnosum* CUPV411 dextran.

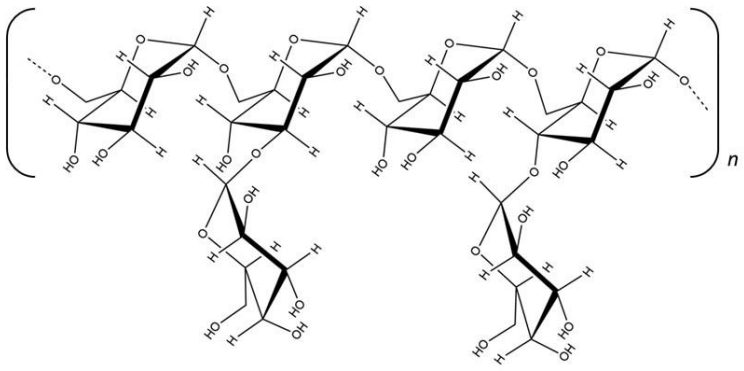

Scheme 1. Representation of the main linkage types of the *Lc. carnosum* CUPV411 dextran. The total number of α-(1→6)-glucopyranose units in the main backbone is represented by *n,* and according to the quantitative data from NMR, this value was 94.4%. Side chains (5.6%), mostly of a single α-glucopyranose unit, partially substitute the α-(1→6) backbone at *O*-3 and *O*-4.

3.2. Detection of dextran production by *L. mali* CUPV271 and *Lc. carnosum* CUPV411

Dextrans are synthesized by dextransucrases using sucrose as substrate (Kothari, Das, Patel, & Goyal, 2014). Thus, for a macroscopic detection of the dextrans synthesized by the two LAB, the bacteria were grown in MRSS-agar plates. In addition, plates containing MRSG-agar were also inoculated as negative controls. As expected, after growth for 48 h in the presence of sucrose the colonies of both strains were mucoid whereas the colonies generated in MRSG medium did not show this phenotype. Moreover, both LAB developed colonies with a larger size upon growth in MRSS medium (Figure 6). Finally, comparing the colonies of both LAB grown in the presence of sucrose some differences were observed. The CUPV271 strain presented convex colonies firmly adhered to the agar even after 264 h of incubation. On the contrary, CUPV411 colonies were flatter and with less adherence to the agar. This difference in colonies' morphology has also been described for other dextran-producing LAB (Zarour et al., 2017).

Analysis of the two LAB by TEM (inset in Figure 7) confirmed the presence of the EPS attached or surrounding the bacteria in cultures grown in MRSS and not MRSG.

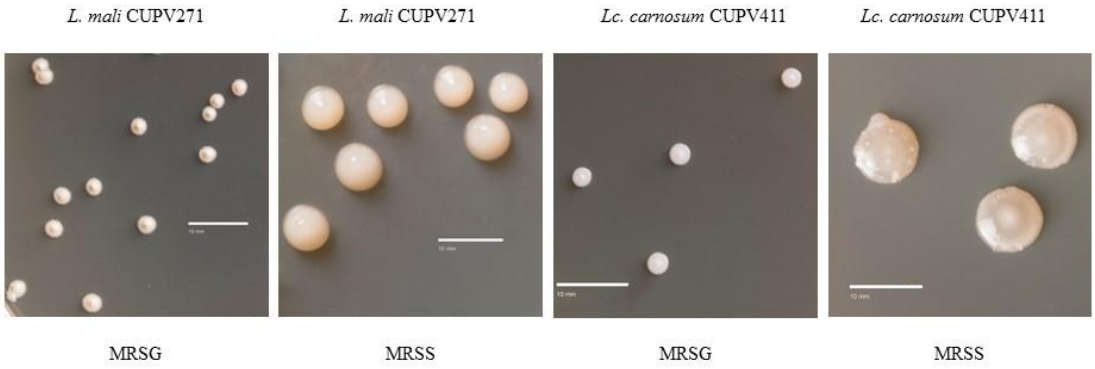

Fig. 6. Detection of EPS production by LAB on solid media. Bacterial colonies in MRSG and MRSS after 240 h of incubation.

3.3. Capacity of *L. mali* CUPV271 and *Lc. carnosum* CUPV411 to adhere to Caco-2 cells

As we have previously observed in some dextran-producing bacteria, the differences in the colonies' morphology correlate with different capacities to bind enterocytes in the presence or absence of EPS (Nácher-Vázquez et al, 2017; Zarour et al., 2017).

Therefore, we tested the adhesion capacity of the LAB grown in media with or without sucrose (MRSS or MRSG) in an *in vitro* assay, measuring the binding of the bacteria to human epithelial Caco-2 cells (Figure 7). The adhesion capacity of *Lc. carnosum* CUPV411 (2.73 ± 0.15%) did not change regardless of the presence or absence of dextran in the medium, which coincides with the results reported for several *Leuconostoc* strains. On the other hand, the adherence to eukaryotic cells of *L. mali* CUPV271 was significantly reduced from 2.85% ± 0.14% to 0.86 ± 0.07% in conditions allowing dextran synthesis. These results are in accordance with those reported for the dextran-producing *L. sakei* MN1 (Nácher-Vázquez et al, 2017). However, it should be stated that sometimes the HoPS produced by LAB also enhance the bacterial binding capacity, as previously reported for the β–glucan produced by *Pediococcus parvulus* strains (Fernández de Palencia et al., 2009; Garai-Ibabe et al., 2010).

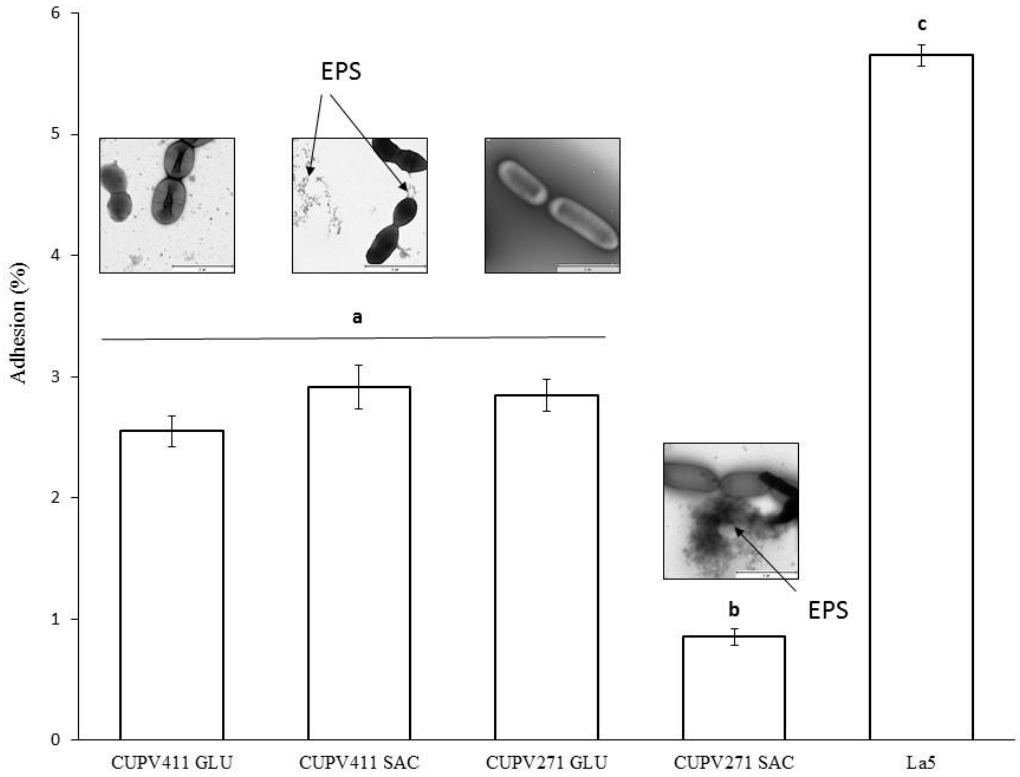

Fig. 7. Adhesion of LAB strains to Caco-2 cells. Adhesion levels are expressed as the percentage of cfu. Data were analyzed by ANOVA. Differences (a-c) were significant with a *$p \leq 0.05$.

3.4. Physicochemical characterization of the dextrans

The results presented in sections 3.2 and 3.3 indicated differences between the dextrans synthesized by *L. mali* CUPV271 and *Lc. carnosum* CUPV411. However, the chemical analyses described in section 3.1 showed that both dextrans had similar primary structure and branching degrees. Therefore, with the aim of elucidating whether some significant differences existed between both dextrans, they were subjected to a deeper physicochemical characterization.

3.4.1. Molar mass distribution

The weight average molar mass (M_w), weight average radius of gyration (R_w), coefficient υ ($\log R_w/\log M_w$) and polydispersity index (PDI, M_w/M_n) of the two isolated EPS were determined by SEC-MALLS. Chromatograms are depicted in Figure 7 and parameters are summarized in Table 3. The chromatogram of the dextran produced by *L. mali* CUPV271 (Fig. 8A) showed a M_w of 1.23 x 10^8 g/mol, corresponding to a low polydispersity (1.05), very close to monodispersity. The M_w of the EPS of *Lc. carnosum* CUPV411 (Fig. 8B), was in the same log order, 3.58 x 10^8 g/mol, and showed a moderate polydispersity (1.25). This peak is being considered as a sole distribution of M_w. However, the presence of another slightly small distribution could have been assigned by the deformation at the left side of the peak. Moreover, it could be interpreted as a shoulder, which might be due to the mixture of aggregates and single molecular structures co-eluting under the same peak, as reported before (Maina et al., 2014). Nevertheless, this would not be clearly stated unless a column with more resolution at higher M_w levels is used.

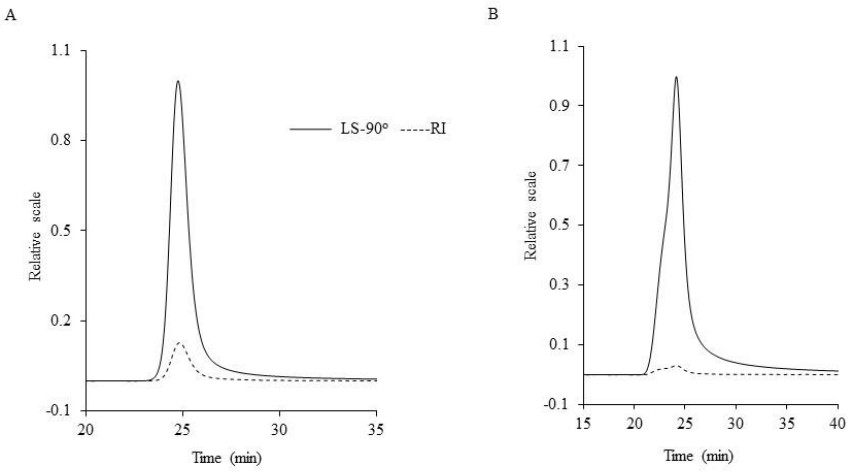

458 **Fig. 8. Size exclusion chromatography (SEC) analysis of the EPS synthesized by**
459 **the studied strains.** (A) EPS produced by *Leuconostoc carnosum* CUPV411 and (B)
460 EPS isolated from *Lactobacillus mali* CUPV271. The figure shows two chromatograms
461 where the continuous line corresponds to the multi-angle laser light scattering (MALLS)
462 detector, set at an angle of 90°, and the dashed line corresponds to the refraction index
463 (RI) detector.
464
465
466 **Table 3.** Physicochemical characteristics of the dextrans produced by *Lc. carnosum*
467 CUPV411 and *L. mali* CUPV271.

	Mean ±SD (n=2)	
	CUPV271	**CUPV411**
Elution time (min)	25.6 ± 0.04	24.9 ± 0.04
Amount (mg/50 µL)	223.4 ± 24.4	106.9 ± 6.7
M_w (g/mol)	1.23E+08 ± 2.6E+06	3.58E+08 ± 1.61E+07
Polydispersity (M_w/M_n)	1.05 ± 0.08	1.25 ± 0.02
R_w (nm)	63.55 ± 0.64	163.65 ± 2.19
υ (log R_w/log M_w)	0.22 ± 2.62E-04	0.26 ± 6.55E-05

468 M_w, weight average molar mass; R_w, weight average radius of gyration.
469
470

3.4.2. Thermal degradation

The patterns of thermal degradation of the two dextrans in aerobic and anoxic atmospheres were analyzed by TGA. Table 4 shows the thermal decomposition temperatures for 5% and 50% weight loss ($T_{5\%}$ and $T_{50\%)}$, the temperature of maximum loss rate (T_{max}) and the fraction of solid residue at 580 ^{o}C of the thermograms obtained in nitrogen and air atmospheres.

Table 4. TGA data for the dextrans isolated from *Lc. carnosum* CUPV411 and *L. mali* CUPV271.

	T_5 (°C)		T_{50} (°C)		T_{max} (°C)			Residue (%)	
Sample	*In N_2*	*In O_2*	*In N_2*	*In O_2*	*In N_2* [a]	*In O_2*		*In N_2*	*In O_2*
CUPV411	80	83	301	305	287	288 [a]	497 [b]	21.1	1.1
CUPV271	90	85	311	310	305	304 [a]	489 [b]	14.1	0.6

[a]Second or third stage for CUPV271 or CUPV411, respectively.

[b]Third or fourth stage for CUPV271 or CUPV411, respectively.

The TGA curves presented in Figure 9 indicate that degradation in anoxic conditions of the polymers of *Lc. carnosum* CUPV411 (Figure 9A, black graph) and *L. mali* CUPV271 (Figure 9B, black graph) took place in three and two steps, respectively. In the first stage, weight loss was observed at similar temperature range for both dextrans (between 25 and 115 °C) and amounted to *ca.* 5%. This loss might be due to the evaporation of the water embedded in the polymers, which are very hygroscopic. However, it could also be due to the evaporation of the ethanol used for the precipitation of the dextrans, as previously reported (Zamora et al., 2002). The second degradation stage corresponded to the decomposition of the polymeric chain, accompanied by the rupture of C-C and C-O bonds, generating CO, CO_2 and water, as reported before (Kenari, Imani, & Nodehi, 2013; Miao et al., 2015). It was characterized by severe weight losses for both dextrans: 55% (from 226 to 333 °C) for CUPV411, and 78% (from 229 to 441 °C) for CUPV271. A third stage of degradation was observed for the dextran of CUPV411, which consisted of a 14% weight loss (from 333 to 465 °C). In the end, a char residue from both dextrans was formed, corresponding to a carbonaceous or polynuclear aromatic structure.

The thermal degradation of both dextrans in aerobic conditions (Figure 9A and B, grey graphs) was carried out in three and four steps for CUPV271 and CUPV411, respectively. The first stage was again characterized by a weight loss of 5% due to the evaporation of embedded water and remaining ethanol (below 105 °C). A second stage where the majority of the depolymerization was carried out, was outlined by dramatic weigh losses of 51% (from 219 to 322 °C) for CUPV411 and 72% (from 221 to 401 °C) for CUPV271. At the end of this degradation phase, a little shoulder was observed in the curve corresponding to the dextran from *L. mali*, which was not considered as a whole stage itself, and which implied a weight loss of around 8% (341-401 °C). On the contrary, *Lc. carnosum* dextran experimented a third phase of thermal degradation in which a 14% weight loss occurred (between 322 and 389 °C). Finally, the last phase of degradation for both dextrans, only present in the aerobic atmosphere, was due to the oxidative degradation of the carbonaceous structure formed in the previous stages. It caused 28% and 21% weight losses for CUPV411 and CUPV271 dextrans, respectively. Therefore, the thermal degradation of the two dextrans was slightly different, since an additional step was observed for that of *Lc. carnosum* CUPV411 in both atmospheres which, according to the methylation data (Table 1), has more branching points in α-(1,3). However, this is not sufficient to explain the results obtained *in vivo* with the producing LAB. Nevertheless, the high degradation temperatures obtained for both dextrans, either in anoxia or in the presence of oxygen, would mean an advantage for application in the food industry.

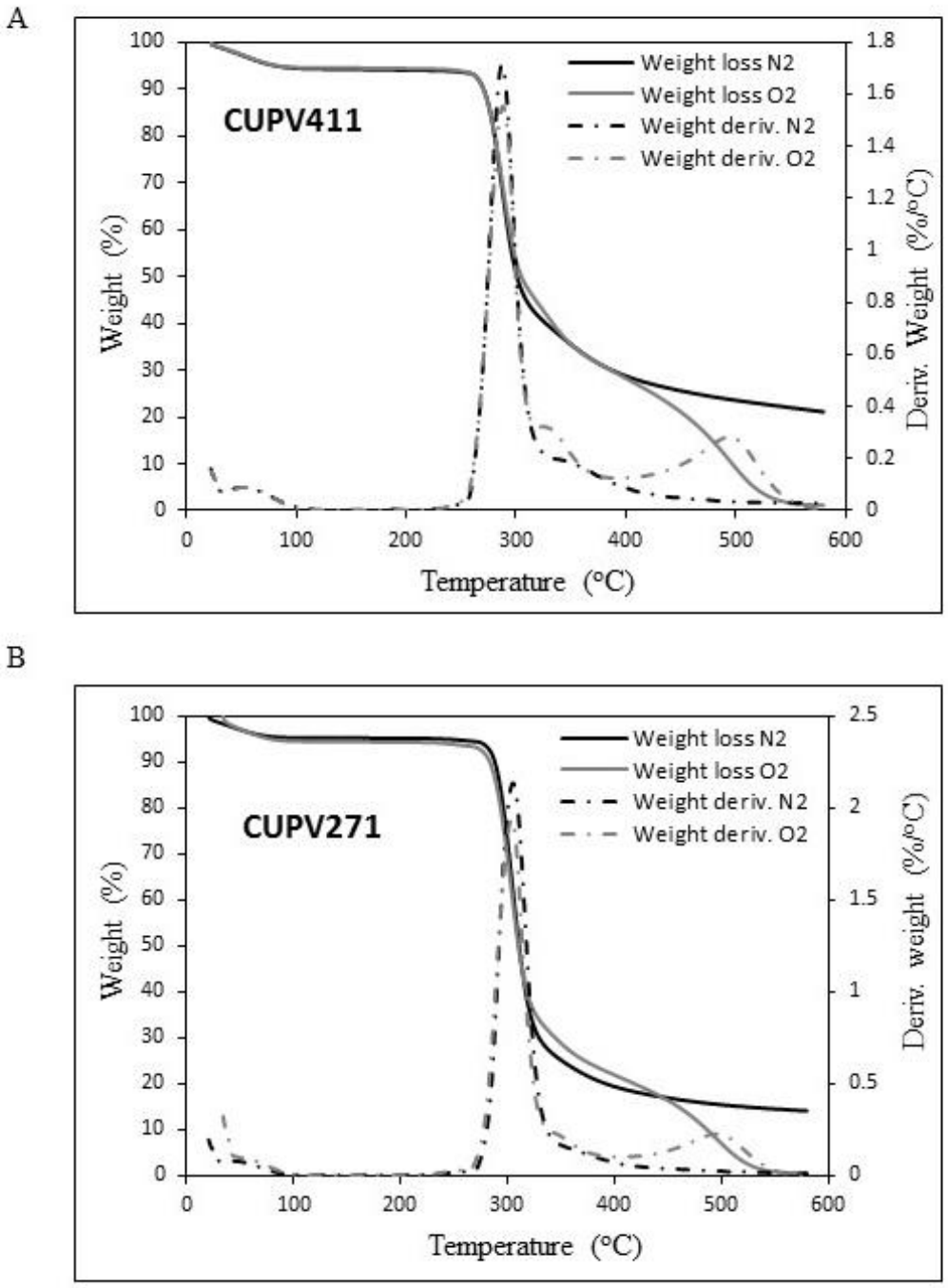

525

526 **Fig. 9. TGA curves.** Thermal degradation of the EPS of (A) *Leuconostoc carnosum*
527 CUPV411 and (B) *Lactobacillus mali* CUPV721. Black lines correspond to nitrogen
528 atmosphere and grey lines correspond the oxidative degradation. Continuous line refers
529 to the weight loss expressed in percentage, and dashed line represents the weight
530 derivative, expressed in %/°C.

531

532

3.4.3. Thermal properties

The degree of crystallinity of the dextrans was evaluated by differential scanning calorimetry. Figure 10 depicts two heating scans of the samples. The first one (Figure 10A), shows a broad endothermal peak around 115 °C for both dextrans, which is due to evaporation of the water embedded in the polymers, as described by other authors (Zhang & Chu, 2002). The glass transition temperature (T_g), measured in the last scan, was taken as the inflection point of the heat capacity change (Irague et al., 2012). The T_g values of the polysaccharides were 225.7 °C (CUPV411) and 226.8 °C (CUPV271), which are close to those reported for dextrans (Rosca et al., 2018). These high T_g are attributed to the presence of strong hydrogen bonds in these polymers (dos Santos Campos, Lopes Cassimiro, Spirandeli Crespi, Emília Almeida, & Daflon Gremião, 2013; Zhang & Chu, 2002).

No exothermic peaks have been observed with these dextrans, thus no melting temperature was obtained. In addition, no crystallization peaks were seen in the cooling stage. Therefore, these results suggest an amorphous behavior for the dextrans studied, as previously reported for other dextrans (dos Santos Campos et al., 2013; Zhang & Chu, 2002).

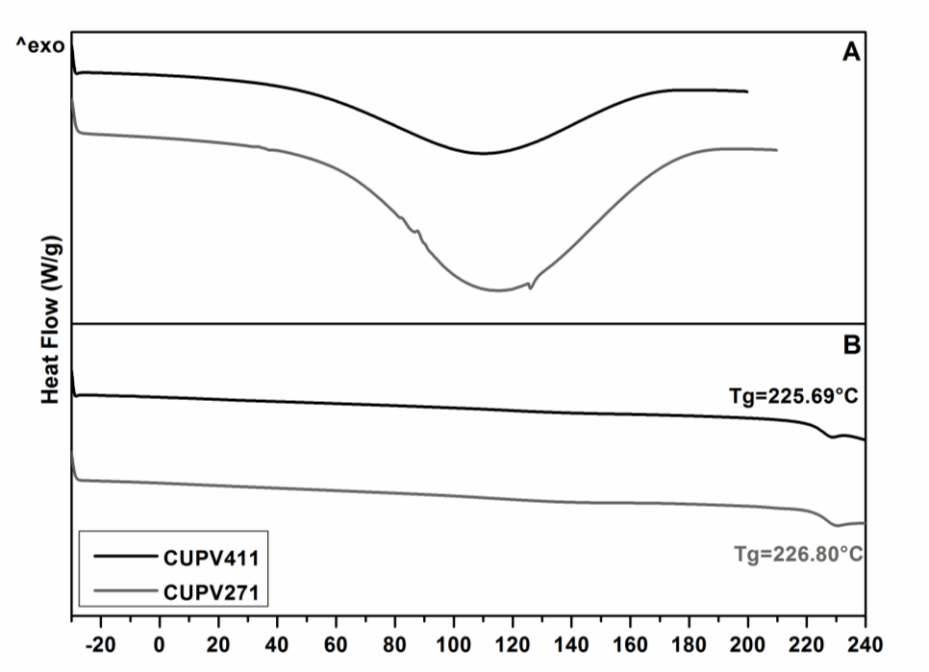

Fig. 10. DSC curves. Black lines for CUPV411 strain and grey ones for CUPV271 strain. (A) First heating scan from -30 °C to 210 °C. (B) Second heating scan in which the glass transition temperature (T_g) of each EPS is observed.

3.4.4. X-ray diffraction of dextrans

Despite the fact that in the DSC analysis no exothermic peaks were observed, there is a remote possibility for dextrans to form crystals in their structure. The degradation temperature under nitrogen atmosphere was *ca.* 220 °C for both dextrans, thus, if the melting temperature was higher than the degradation temperature, the exothermic peak indicating the melting of the crystals would not be observed by DSC. X-ray diffraction was carried out to check this possibility. Figure 11 shows the diffraction profiles of dextrans produced by *L. mali* CUPV271 and *Lc. carnosum* CUPV411, confirming the amorphous structure of the polymers. However, a blunt peak appears in the profile of both dextrans in the 2θ range of 15-25º, indicating a small amount of the sample with some level of crystallinity, as reported previously (Yuan et al., 2009). Thus, no differences were found in the formation of crystals between the two dextrans under study.

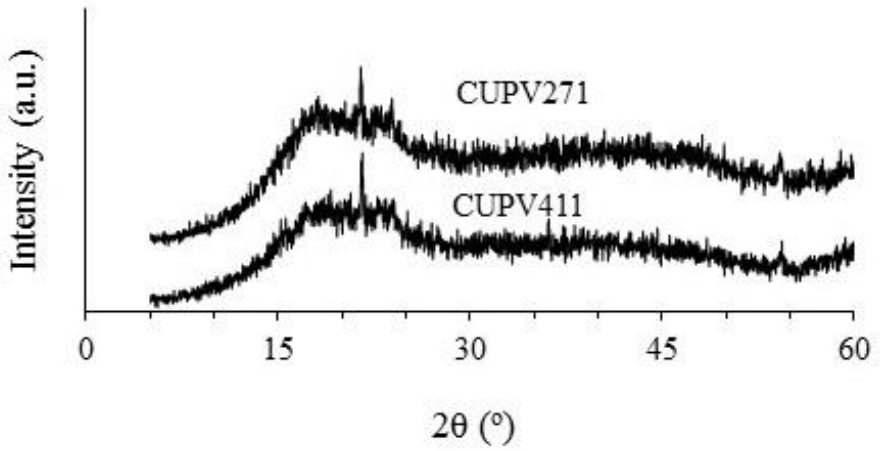

Fig. 11. X-ray diffraction diagrams of dextran produced by *L. mali* CUPV271 (up) and by *Lc. carnosum* CUPV411 (down).

3.4.5. Atomic force micrographs of dextrans

Finally, atomic force was used to see if differences in the spatial conformation of the dextrans existed. As also reported for the EPS produced by other *Lactobacillus* species (Ahmed, Wang, Anjum, Ahmad, & Khan, 2013; Wang et al., 2010), the AFM images (height and phase) of the dextran produced by *L. mali* (Figure 12A) revealed a mixture of irregular rounded lumps with few random linear chains, which become visible when saturating to the maximum the image. These fibrillary structures were more evident in the phase micrograph, suggesting that they were thinner than the aggregates and

578 composed of less material. The lumps were very different in shape and size, ranging
579 from 0.13 to 0.54 μm, whereas the stretched material formed clusters of chains yielding
580 0.033 ±0.004 μm of width. On the contrary, irregular big aggregates ranging from 0.35
581 to 0.67 μm, and spherical small lumps with a diameter <0.1 μm, were observed for the
582 dextran isolated from *Lc. carnosum* (Figure 12B), as previously described for the
583 dextran produced by *Leuconostoc lactis* KC117496 (Saravanan & Shetty, 2016).
584 Moreover, the molecules from both polymers seemed to be tightly packed, suggesting a
585 pseudoplastic behavior with strong affinity for water molecules (Ahmed et al., 2013;
586 Wang et al., 2010), which was further confirmed with rheology assays.
587

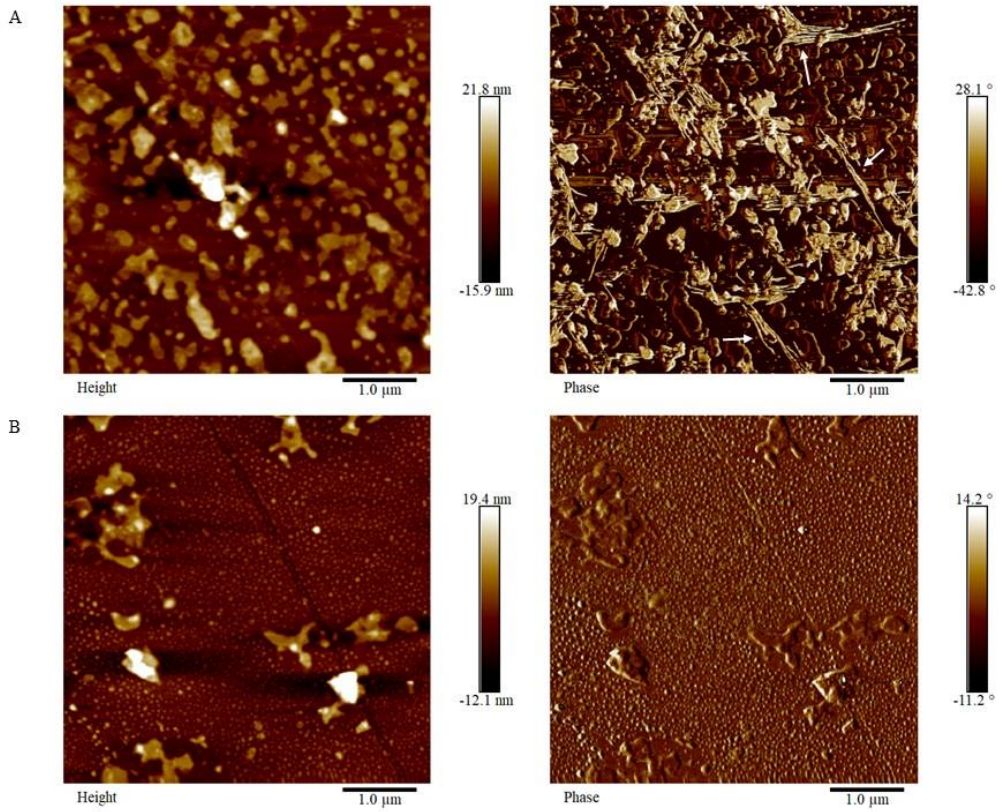

588

589 **Fig. 12.** Height (left) and phase (right) AFM planar images of dextrans synthesized by
590 *L. mali* CUPV271 (A) and *Lc. carnosum* CUPV411 (B). White arrows in the phase
591 micrograph of the dextran produced by CUPV271 indicates the fibrillary morphology.
592
593
594

Taking together the results obtained in the different characterization assays, both dextrans present slight differences in their size or percentage of ramifications, although atomic force micrographs showed some differences at supramolecular level. Thus, the different spatial distribution of the dextrans might be on the basis of the different behaviors observed *in vivo*.

3.5. Rheological properties of dextrans produced by LAB

Since atomic force microscopy suggested the possible pseudoplastic behavior for the dextrans studied, we evaluated their flow behavior in solution, under shear at a constant temperature. The performance of the two dextrans was similar and coincided with that previously described for these type of polymers (Vuillemin et al., 2018; Zarour et al., 2017). Then, only the viscosity curves for the dextran of *L. carnosum* CUPV411 will be represented. An ideally viscous or Newtonian flow behavior was observed at low concentrations (up to a 0.5%), in which the viscosity remained constant over the entire shear rate range (Figure 13). This viscosity was the same as in resting conditions (zero-shear viscosity, η_o). However, at higher concentrations, a shear-thinning or pseudoplastic flow behavior was observed, in which the viscosity decreased with increasing share rates. The hydrodynamic forces generated during the shear could have led to the breakdown of the structural units and the physical networks between the dextrans' chains, as reported before (Prasanna, Bell, Grandison, & Charalampopoulos, 2012; Zarour et al., 2017). Pseudoplastic characteristics of a polymer are not uniform in the whole range of shear rates. This behavior is characterized by showing a plateau value of the zero-shear viscosity η_o at low shear rates below 1 s^{-1}. In this case, measures in the range of 0-1 s^{-1} were limited by the characteristics of the instrument used. Therefore, an extrapolation by the Cross model was applied in order to obtain the η_o value with the aim of comparing the viscosity of the two dextrans in a status near to the rest. At a given concentration of 5%, a higher plateau value of zero-shear viscosity was observed for dextran produced by *Lc. carnosum* CUPV411 (19.56 Pas) than that for the one produced by *L. mali* CUPV271 (0.09 Pas), indicating a higher average molar mass for the former dextran, as confirmed by SEC-MALLS.

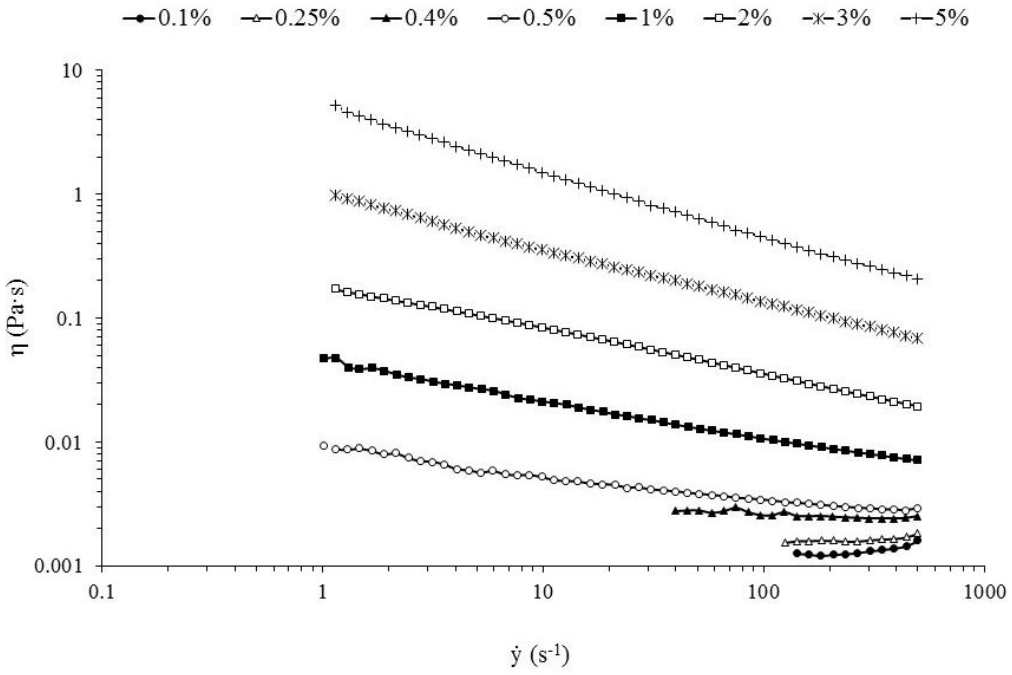

Fig. 13. Double logarithmic plot of viscosity curves of dextrans isolated from LAB. Viscosity curves for dextran isolated from *Leuconostoc carnosum* CUPV411 obtained by measuring aqueous solutions at different concentrations in a viscoelastometer.

The critical concentration, defined as the concentration of a polymer at which the equivalent sphere of a given polymer molecule just touches the equivalent spheres of all of its nearest neighbor molecules (Kulicke & Clasen, 2004), was calculated for both dextrans (Figure 14). The data recorded suggested an increase in the Newtonian viscosity with the polymer's concentration. The critical concentration for the dextran from *L. mali* was 3.8%, while for that from *Lc. carnosum* it was 0.4%. These values are very related to the entanglements occurring both inside a single molecule and between different molecules. Therefore, the less-branched dextran produced by *L. mali* CUPV271 (Table 1) would require more molecules to reach the same number of entanglements than the polymer from *Lc. carnosum* CUPV411, which justifies its higher critical concentration.

The shear-thinning data presented above suggest that the dextrans studied would be very suitable to improve the texture or palatability of new fermented products.

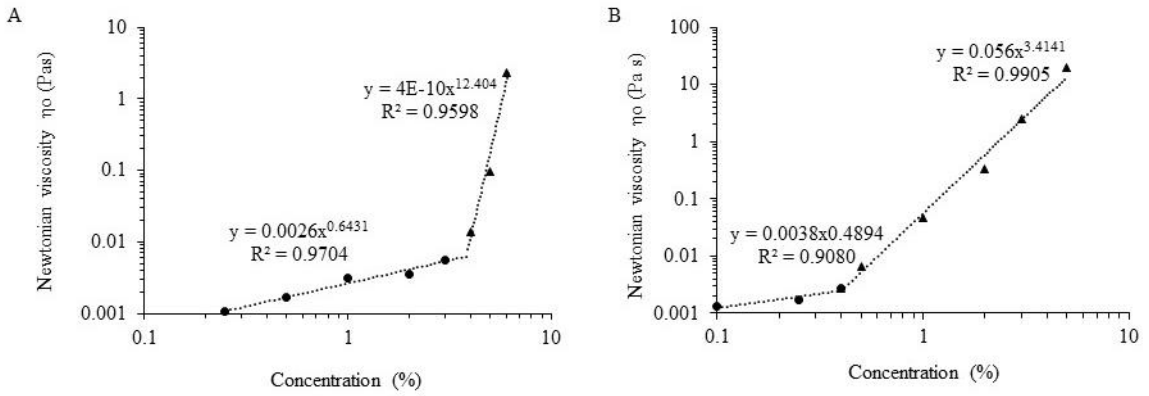

Fig. 14. Calculation of the critic concentration of the dextrans studied. Representation in a double logarithmic plot of the Newtonian viscosity versus the concentration expressed in percentage of (A) *L. mali* CUPV271 strain and (B) *L. carnosum* CUPV411 strain.

3.6. Dextran yield

As far as our knowledge is concerned, it is the first time that EPS are isolated from *L. mali* and *Lc. carnosum* species. The isolation of the dextrans from the culture supernatants was only possible when sucrose and not glucose was present in the media, as it has been reported by other authors for dextran-producing LAB (Nácher-Vázquez et al., 2017; Zarour et al., 2017). The recovery of the EPS after 48 h of incubation in SMDS (2% sucrose), measured by the phenol-sulphuric acid method, was 3.65 ± 0.21 g/L for *Lc. carnosum* CUPV411, similar to the 1.25 ± 0.04 g/L described for *Lc. mesenteroides* RTF10 grown for 13 h in CDMS (0.8% sucrose) (Nácher-Vázquez et al., 2017). For *L. mali* CUPV271 the recovery was higher than for CUPV411 in the same conditions, yielding 11.65 ± 1.15 g/L. This concentration exceeded the 2.20 ± 0.09 g/L produced by *L. sakei* MN1 after 13 h of incubation in CDMS (Nácher-Vázquez et al., 2017). Some species from *Oenococcus* have also been reported to produce EPS. In particular, the strain *O. oeni* S11, isolated from alcoholic beverages (sparkling white wine) in France, produced 3.87 ± 0.02 g/L of dextran in SMDS (1% sucrose) after a two-week incubation period (Dimopoulou et al., 2014). Thus, the overall results indicate a potential industrial use of the dextrans studied here, although their production levels are well below the 154 g/L reported for *Lc. mesenteroides* NRRL B-512F at optimized conditions for batch fermentation (Karthikeyan, Rakshit, & Baradarajan, 1996).

Considering that neither the medium nor the culture conditions have been optimized in the current work, the perspective for production's improvement is high, supporting the potential use of the *L. mali* CUPV271 dextran for industrial purposes.

4. Conclusions

As far as we know, the EPSs produced by *Lc. carnosum* and *L. mali* strains have been purified and characterized for the first time. Chemical and spectroscopic analyses revealed that both polymers are *O*-3- and *O*-4-branched dextrans, whose presence affected differentially to the adhesion capacity of the producing LAB. This differential pattern could be due to differences in their supramolecular structures, as deduced from AFM. In addition, these dextrans are amorphous and presented a pseudoplastic behavior. This shear-thinning property may confer them an advantage in the food industry for improving sensory properties as mouth feel and flavor release. In addition, they would be very suitable for mixing, pouring or pumping, very common processes in the industry. Moreover, *L. mali* CUPV271 produces a considerably higher amount of polymer than *Lc. carnosum* CUPV411, thus, it might be a strong candidate for optimization aimed to the future development of food, producing the dextran *in vivo*, or being included in the product as an additive.

5. Acknowledgements

We thank Dr. Guillermo Padilla Alonso for his valuable assistance in the bio-statistical analysis and Dr. Stephen Elson for the critical reading of the manuscript. Technical and human support by Dr. Aitor Larrañaga, (X-ray Facility) and Dr. Loli Martín (Materials and Surfaces – Macrobehavior Facility) from the general research service (SGIker) of the University of Basque Country (UPV/EHU) is also gratefully acknowledged. Finally, the valuable assistance of Dr. Mª Eugenia Muñoz (POLYMAT-Rheology group) is also acknowledged.

6. Declaration of interest statement

None.

7. Funding

This work was supported by a grant from de Department of Environment, Territorial Planification, Agriculture and Fishing from the Basque Government, by the Provincial Council of Gipuzkoa (Exp. 77/17) and by the Spanish Ministry of Science and Innovation (AGL 2015-65010-C3-1-R).

8. References

Ahmed, Z., Wang, Y., Anjum, N., Ahmad, A., & Khan, S. T. (2013). Characterization of exopolysaccharide produced by *Lactobacillus kefiranofaciens* ZW3 isolated from Tibet kefir - Part II. *Food Hydrocolloids*, *30*(1), 343–350. https://doi.org/10.1016/j.foodhyd.2012.06.009

BeMiller, 2003. Dextran. In: Encyclopedia of Food Sciences and Nutrition (Second Edition), Luiz Trugo and Paul M. Finglas (Eds), Academic Press, Cambridge Massachusetts, pp. 1772-1773. https://doi.org/10.1016/B0-12-227055-X/00330-8

Chang, R. L. S., Crawford, M. P., & West, M. D. (1980). An assessment of the potential use of anionic dextrans as a plasma substitute. *Journal of Biomedical Engineering*, *2*(1), 41–44. https://doi.org/10.1016/0141-5425(80)90090-4

Cheetham, N. W. H., Fiala-Beer, E., & Walker, G. J. (1990). Dextran structural details from high-field proton NMR spectroscopy. *Carbohydrate Polymers*, *14*(2), 149-158. https://doi.org/10.1016/0144-8617(90)90027-P

Ciucanu, I., & Kerek, F. (1984). A simple and rapid method for the permethylation of carbohydrates. *Carbohydrate Research 13*, 209–217. https://doi.org/10.1016/0008-6215(84)85242-8

Corcuera, M. A., Rueda, L., Fernandez D'Arlas, B., Arbelaiz, A., Marieta, C., Mondragon, I., & Eceiza, A. (2010). Microstructure and properties of polyurethanes derived from castor oil. *Polymer Degradation and Stability*, *95*(11), 2175–2184. https://doi.org/10.1016/j.polymdegradstab.2010.03.001

Cross, M. M. (1965). Rheology of non-Newtonian fluids: A new flow equation for pseudoplastic systems. *Journal of Colloid Science*, *20*(5), 417–437. https://doi.org/10.1016/0095-8522(65)90022-X

De Man, J. C., Rogosa, M., & Sharpe, M. E. (1960). A medium for the cultivation of lactobacilli. *Journal of Applied Bacteriology*, *23*(1), 130–135. https://doi.org/10.1111/j.1365-2672.1960.tb00188.x

Dertli, E., Colquhoun, I. J., Côté, G. L., Le, G., & Narbad, A. (2018). Structural analysis of the α-D-glucan produced by the sourdough isolate *Lactobacillus brevis* E25.

Food Chemistry, *242*(June 2017), 45–52. https://doi.org/10.1016/j.foodchem.2017.09.017

Dimopoulou, M., Vuillemin, M., Campbell-Sills, H., Lucas, P. M., Ballestra, P., Miot-Sertier, C., Favier, M., Coulon, J., Moine, V., Doco, T., Roques, M., Williams, P., Petrel, M., Gontier, E., Moulis, C., Remaud-Simeon, M., & Dols-Lafargue, M. (2014). Exopolysaccharide (EPS) synthesis by *Oenococcus oeni*: from genes to phenotypes. *PLoS ONE*, *9*(6), 1–15. https://doi.org/10.1371/journal.pone.0098898

dos Santos Campos, F., Lopes Cassimiro, D., Spirandeli Crespi, M., Emília Almeida, A., & Daflon Gremião, M. P. (2013). Preparation and characterisation of Dextran-70 hydrogel for controlled release of praziquantel. *Brazilian Journal of Pharmaceutical Sciences*, *49*(1), 75–83. https://doi.org/10.1590/S1984-82502013000100009

Dubois, M., Gilles, K., Hamilton, J., Rebers, P., & Smith, F. (1956). Colorimetric method for determination of sugars and related substances. *Analytical Chemistry*, *28*(3), 350–356. https://doi.org/10.1021/ac60111a017

Dueñas-Chasco, M. T., Rodríguez-Carvajal, M. A., Tejero-Mateo, P., Espartero, J. L., Irastorza-Iribas, A., & Gil-Serrano, A. M. (1998). Structural analysis of the exopolysaccharides produced by *Lactobacillus* spp . G-77. *Cancer Research*, *307*, 125–133. https://doi.org/10.1016/S0008-6215(98)00034-2

Dueñas-Chasco, M. T., Rodríguez-Carvajal, M. A., Tejero Mateo, P., Franco-Rodríguez, G., Espartero, J. L., Irastorza-Iribas, A., & Gil-Serrano, A. M. (1997). Structural analysis of the exopolysaccharide produced by *Pediococcus damnosus* 2.6. *Carbohydrate Research*, *303*, 453–458. https://doi.org/10.1016/S0008-6215(97)00192-4

Fernández, M. D., Fernández, M. J., & Cobos, M. (2016). Effect of polyhedral oligomeric silsesquioxane (POSS) derivative on the morphology, thermal, mechanical and surface properties of poly(lactic acid)-based nanocomposites. *Journal of Materials Science*, *51*(7), 3628–3642. https://doi.org/10.1007/s10853-015-9686-5

Fernández de Palencia, P., Werning, M. L., Sierra-Filardi, E., Dueñas, M. T., Irastorza, A., Corbí, A. L., & López, P. (2009). Probiotic properties of the 2-substituted (1,3)-β-D-glucan-producing bacterium *Pediococcus parvulus* 2.6. *Applied and Environmental Microbiology*, *75*(14), 4887–4891. https://doi.org/10.1128/AEM.00394-09

Fraga Vidal, R., Moulis, C., Escalier, P., Remaud-Siméon, M., & Monsan, P. (2011). Isolation of a gene from *Leuconostoc citreum* B/110-1-2 encoding a novel dextransucrase enzyme. *Current Microbiology*, *62*(4), 1260–1266. https://doi.org/10.1007/s00284-010-9851-7

Garai-Ibabe, G., Dueñas, M. T., Irastorza, A., Sierra-Filardi, E., Werning, M. L., López, P., Corbí, A. L., & Fernández de Palencia, P. (2010). Naturally occurring 2-substituted (1,3)-β-D-glucan producing *Lactobacillus suebicus* and *Pediococcus parvulus* strains with potential utility in the production of functional foods. *Bioresource Technology*, *101*(23), 9254–9263. https://doi.org/10.1016/j.biortech.2010.07.050

Heyn, A. N. J. (1974). The infrared absorption spectrum of dextran and its bound water. *Biopolymers*, *13*(3), 475–506. https://doi.org/10.1002/bip.1974.360130304

Hu, Y., & Gänzle, M. G. (2018). Effect of temperature on production of oligosaccharides and dextran by *Weissella cibaria* 10 M. *International Journal of Food Microbiology*, *280*(January), 27–34. https://doi.org/10.1016/j.ijfoodmicro.2018.05.003

Icoz, D. Z., & Kokini, J. L. (2007). Probing the boundaries of miscibility in model carbohydrates consisting of chemically derivatized dextrans using DSC and FTIR spectroscopy. *Carbohydrate Polymers*, *68*(1), 68–76. https://doi.org/10.1016/j.carbpol.2006.07.011

Irague, R., Rolland-Sabaté, A., Tarquis, L., Doublier, J. L., Moulis, C., Monsan, P., Remaud-Siméon, M., Potocki-Véronèse, G., & Buléon, A. (2012). Structure and property engineering of α-D-glucans synthesized by dextransucrase mutants. *Biomacromolecules*, *13*(1), 187–195. https://doi.org/10.1021/bm201453r

Karthikeyan, R. S., Rakshit, S. K., & Baradarajan, A. (1996). Optimization of batch fermentation conditions for dextran production. *Bioprocess Engineering*, *15*(5), 247–251. https://doi.org/10.1007/BF02391585

Kenari, H. S., Imani, M., & Nodehi, A. (2013). Full factorial design-of-experiments for preparation of crosslinked dextran microspheres. *Journal of Applied Polymer Science*, *127*(5), 3712–3724. https://doi.org/10.1002/app.37983

Kothari, D., Das, D., Patel, S., & Goyal, A. (2014). Dextran and food application. In K. Gopal Ramawat & J.-M. Mérillon (Eds.), *Polysaccharides*. Switzerland: Springer International Publishing. https://doi.org/10.1007/978-3-319-03751-6

Kulicke, W. M., & Clasen, C. (2004). *Viscosimetry of polymers and polyelectrolytes*.

(C. Clasen, Ed.). Springer.

Lakshmi Bhavani, A., & Nisha, J. (2010). Dextran - The polysaccharide with versatile uses. *International Journal of Pharma and Bio Sciences*, *1*(4), 569–573.

Maina, N. H., Pitkänen, L., Heikkinen, S., Tuomainen, P., Virkki, L., & Tenkanen, M. (2014). Challenges in analysis of high-molar mass dextrans: Comparison of HPSEC, AsFlFFF and DOSY NMR spectroscopy. *Carbohydrate Polymers*, *99*, 199–207. https://doi.org/10.1016/j.carbpol.2013.08.021

Meng, X., Gangoiti, J., Bai, Y., Pijning, T., Van Leeuwen, S. S., & Dijkhuizen, L. (2016). Structure–function relationships of family GH70 glucansucrase and 4,6-α-glucanotransferase enzymes, and their evolutionary relationships with family GH13 enzymes. *Cellular and Molecular Life Sciences*, *73*(14), 2681–2706. https://doi.org/10.1007/s00018-016-2245-7

Miao, M., Huang, C., Jia, X., Cui, S. W., Jiang, B., & Zhang, T. (2015). Physicochemical characteristics of a high molecular weight bioengineered α-D-glucan from *Leuconostoc citreum* SK24.002. *Food Hydrocolloids*, *50*, 37–43. https://doi.org/10.1016/j.foodhyd.2015.04.009

Miao, M., Jia, X., Jiang, B., Wu, S., Cui, S. W., & Li, X. (2016). Elucidating molecular structure and prebiotics properties of bioengineered α-D-glucan from *Leuconostoc citreum* SK24.002. *Food Hydrocolloids*, *54*, 227–233. https://doi.org/10.1016/j.foodhyd.2015.10.013

Nácher-Vázquez, M., Ballesteros, N., Canales, Á., Rodríguez Saint-Jean, S., Pérez-Prieto, S. I., Prieto, A., Aznar, R., & López, P. (2015). Dextrans produced by lactic acid bacteria exhibit antiviral and immunomodulatory activity against salmonid viruses. *Carbohydrate Polymers*, *124*, 292–301. https://doi.org/10.1016/j.carbpol.2015.02.020

Nácher-Vázquez, M., Iturria, I., Zarour, K., Mohedano, M. L., Aznar, R., Pardo, M. Á., & López, P. (2017). Dextran production by *Lactobacillus sakei* MN1 coincides with reduced autoagglutination, biofilm formation and epithelial cell adhesion. *Carbohydrate Polymers*, *168*, 22–31. https://doi.org/10.1016/j.carbpol.2017.03.024

Naessens, M., Cerdobbel, A., Soetaert, W., & Vandamme, E. J. (2005). *Leuconostoc* dextransucrase and dextran: production, properties and applications. *Journal of Chemical Technology and Biotechnology*, *80*(8), 845–860. https://doi.org/10.1002/jctb.1322

Nikolic, M., López, P., Strahinic, I., Suárez, A., Kojic, M., Fernández-García, M.,

Topisirovic, L., Golic, N., & Ruas-Madiedo, P. (2012). Characterisation of the exopolysaccharide (EPS)-producing *Lactobacillus paraplantarum* BGCG11 and its non-EPS producing derivative strains as potential probiotics. *International Journal of Food Microbiology*, *158*(2), 155–162. https://doi.org/10.1016/j.ijfoodmicro.2012.07.015

Notararigo, S., Nácher-Vázquez, M., Ibarburu, I., Werning, M. L., Fernández de Palencia, P., Dueñas, M. T., Aznar, R., López, P., & Prieto, A. (2013). Comparative analysis of production and purification of homo- and hetero-polysaccharides produced by lactic acid bacteria. *Carbohydrate Polymers*, *94*(1), 57–64. https://doi.org/10.1016/j.carbpol.2012.05.016

Pérez-Ramos, A., Nácher-Vázquez, M., Notararigo, S., López, P., & Mohedano, M. L. (2015). Current and future applications of bacterial extracellular polysaccharides. In V. R. Preedy & R. R. Watson (Eds.), *Probiotics, prebiotics and synbiotics: Bioactive foods in health promotion*. Oxford, UK: Elsevier. https://doi.org/10.1016/B978-0-12-802189-7.00022-8

Polak-Berecka, M., Choma, A., Waśko, A., Górska, S., Gamian, A., & Cybulska, J. (2015). Physicochemical characterization of exopolysaccharides produced by *Lactobacillus rhamnosus* on various carbon sources. *Carbohydrate Polymers*, *117*, 501–509. https://doi.org/10.1016/j.carbpol.2014.10.006

Prasanna, P. H. P., Bell, A., Grandison, A. S., & Charalampopoulos, D. (2012). Emulsifying, rheological and physicochemical properties of exopolysaccharide produced by *Bifidobacterium longum* subsp. *infantis* CCUG 52486 and *Bifidobacterium infantis* NCIMB 702205. *Carbohydrate Polymers*, *90*(1), 533–540. https://doi.org/10.1016/j.carbpol.2012.05.075

Rosca, I., Petrovici, A. R., Peptanariu, D., Nicolescu, A., Dodi, G., Avadanei, M., Ivanov, I. C., Bostanaru, A. C., Mares, M., & Ciolacu, D. (2018). Biosynthesis of dextran by *Weissella confusa* and its *In vitro* functional characteristics. *International Journal of Biological Macromolecules*, *107*, 1765–1772. https://doi.org/10.1016/j.ijbiomac.2017.10.048

Salazar, N., Prieto, A., Leal, J. A., Mayo, B., Bada-Gancedo, J. C., de los Reyes-Gavilán, C. G., & Ruas-Madiedo, P. (2009). Production of exopolysaccharides by *Lactobacillus* and *Bifidobacterium* strains of human origin, and metabolic activity of the producing bacteria in milk. *Journal of Dairy Science*, *92*(9), 4158–4168. https://doi.org/10.3168/jds.2009-2126

Salazar, N., Ruas-Madiedo, P., Prieto, A., Calle, L. P., & de los Reyes-Gavilán, C. G. (2012). Characterization of exopolysaccharides produced by *Bifidobacterium longum* NB667 and its cholate-resistant derivative strain IPLA B667dCo. *Journal of Agricultural and Food Chemistry*, *60*(4), 1028–1035. https://doi.org/10.1021/jf204034n

Saravanan, C., & Shetty, P. K. H. (2016). Isolation and characterization of exopolysaccharide from *Leuconostoc lactis* KC117496 isolated from idli batter. *International Journal of Biological Macromolecules*, *90*, 100–106. https://doi.org/10.1016/j.ijbiomac.2015.02.007

Seymour, F. R., Knapp, R. D., & Bishop, S. H. (1979). Correlation of the structure of dextrans to their ^{1}H-N.M.R. spectra*. *Carbohydrate Research*, *74*, 77–92. https://doi.org/10.1016/S0008-6215(00)86072-3

Seymour, F. R., Knapp, R. D., Chen, E. C. M., Jeanes, A., & Bishop, S. H. (1979). Structural analysis of dextrans containing 2-*O*-α-D-glucosylated α-D-glucopyranosyl residues at the branch points, by use of ^{13}C-nuclear magnetic resonance spectroscopy and gas-liquid chromatography-mass spectrometry. *Carbohydrate Research*, *71*(1), 231–250. https://doi.org/10.1016/S0008-6215(00)84766-7

Torino, M. I., Font de Valdez, G., & Mozzi, F. (2015). Biopolymers from lactic acid bacteria. Novel applications in foods and beverages. *Frontiers in Microbiology*, *6*, 1–16. https://doi.org/10.3389/fmicb.2015.00834

Vuillemin, M., Grimaud, F., Claverie, M., Rolland-Sabaté, A., Garnier, C., Lucas, P., Monsan, P., Dols-Lafargue, M., Remaud-Siméon, M., & Moulis, C. (2018). A dextran with unique rheological properties produced by the dextransucrase from *Oenococcus kitaharae* DSM 17330. *Carbohydrate Polymers*, *179*(September 2017), 10–18. https://doi.org/10.1016/j.carbpol.2017.09.056

Wang, Y., Li, C., Liu, P., Ahmed, Z., Xiao, P., & Bai, X. (2010). Physical characterization of exopolysaccharide produced by *Lactobacillus plantarum* KF5 isolated from Tibet Kefir. *Carbohydrate Polymers*, *82*(3), 895–903. https://doi.org/10.1016/j.carbpol.2010.06.013

Yuan, W., Geng, Y., Wu, F., Liu, Y., Guo, M., Zhao, H., & Jin, T. (2009). Preparation of polysaccharide glassy microparticles with stabilization of proteins. *International Journal of Pharmaceutics*, *366*(1–2), 154–159. https://doi.org/10.1016/j.ijpharm.2008.09.007

911 Zamora, F., González, M. C., Dueñas, M. T., Irastorza, A., Velasco, S., & Ibarburu, I.
912 (2002). Thermodegradation and thermal transitions of an exopolysaccharide
913 produced by *Pediococcus damnosus* 2.6. *Journal of Macromolecular Science -*
914 *Physics*, *41 B*(3), 473–486. https://doi.org/10.1081/MB-120004348
915 Zarour, K., Llamas, M. G., Prieto, A., Ruas-Madiedo, P., Dueñas, M. T., Fernández de
916 Palencia, P., Aznar, R., Mebrouk, K., & López, P. (2017). Rheology and
917 bioactivity of high molecular weight dextrans synthesised by lactic acid bacteria.
918 *Carbohydrate Polymers*, *174*, 646–657.
919 https://doi.org/10.1016/j.carbpol.2017.06.113
920 Zhang, Y., & Chu, C.-C. (2002). Thermal and mechanical properties of biodegradable
921 hydrophilic-hydrophobic hydrogels based on dextran and poly (lactic acid).
922 *Journal of Materials Science: Materials in Medicine*, *13*(8), 773–781.
923 https://doi.org/10.1023/A:1016123125046
924
925